Microchimica Acta (2019) 186: 235
https://doi.org/10.1007/s00604-019-3272-5

ORIGINAL PAPER

A nanocomposite consisting of gold nanobipyramids and multiwalled carbon nanotubes for amperometric nonenzymatic sensing of glucose and hydrogen peroxide

He Mei[1] · **Xuedong Wang**[1] · **Tai Zeng**[1] · **Ling Huang**[1] · **Qun Wang**[1] · **Daoping Ru**[1] · **Tongliang Huang**[1] · **Falin Tian**[2] · **Huimin Wu**[3] · **Jimin Gao**[1]

Received: 22 October 2018 / Accepted: 20 January 2019 / Published online: 12 March 2019

Abstract

Gold nanobipyramids were synthesized by a seed-mediated growth method and then supported by multi-walled carbon nanotubes (denoted as AuNBP/MWCNTs). The electrocatalytic activity of the AuNBP/MWCNTs on a glassy carbon electrode (GCE) towards direct glucose oxidation and hydrogen peroxide reduction was superior to that of AuNBPs and MWCNTs. The modified GCE, operated at a typical working voltage of +0.15 V (vs. SCE) and in 0.1 M NaOH solution, exhibits a linear response in the 10 μM to 36.7 mM glucose concentration range with a 3.0 μM detection limit (at $S/N = 3$) and a sensitivity of 101.2 μA mM^{-1} cm^{-2}. It also demonstrates good sensitivity towards hydrogen peroxide in at pH 7 solution at a working potential of −0.50 V (vs. SCE), with a linear response range from 5.0 μM to 47.3 mM, a sensitivity of 170.6 μA mM^{-1} cm^{-2} and a detection limit of 1.5 μM.

Keywords Nanomaterials · Electrocatalyst · Electrochemical sensor · Non-enzymatic sensor · Cyclic voltammetry · Chronoamperometry · Real sample analysis

Introduction

Quantitative determination of glucose and hydrogen peroxide is in great demand in clinical applications. Enzymatic electrochemical sensor such as test stripes have received extensive attention for its high sensitivity, good selectivity and fast response. But the inherent limitations originated from the intrinsic nature of enzymes such as insufficient stability and reproducibility hinder their further development [1].

To resolve these issues, researchers pay more attention to non-enzymatic electrochemical sensor, which can avoid tedious immobilization procedures of enzyme and offer numerous advantages, such as excellent stability, favorable reproducibility and cost effectiveness [2]. However, compared with enzymatic electrochemical sensor, the selectivity of some non-enzymatic sensors are not suitable for practical application [3]. Therefore, non-enzymatic sensor with excellent electrochemical activity and selectivity are urgently needed. Precious metal nanomaterial, especially Au-based nanoparticles, is of particular interest to fabricate non-enzymatic electrochemical sensor for their excellent conductivity and superior electrocatalytic properties [4]. The gold nanoparticles (AuNPs) [5–7], lamellar-ridge architectured gold (lamellar ridge-Au) [8], gold nanorods (AuNRs) [9, 10], and nanoporous gold [11] have been developed to construct non-enzymatic glucose sensor in alkaline solution. The oxidation of glucose is dependent on the crystalline structures of nanoparticles [12]. Cubic gold nanoparticles with

---

Electronic supplementary material The online version of this article (https://doi.org/10.1007/s00604-019-3272-5) contains supplementary material, which is available to authorized users.

✉ Huimin Wu
whm267@126.com

✉ Jimin Gao
jimingao@yahoo.com

[1] Department of Environmental Sciences, Zhejiang Provincial Key Laboratory of Watershed Science and Health, Wenzhou Medical University, Wenzhou 325035, People's Republic of China

[2] Wenzhou Institute of Biomaterials and Engineering, Chinese Academy of Sciences, Wenzhou 325001, People's Republic of China

[3] Hubei Collaborative Innovation Center for Advanced Organic Chemical Materials & Key Laboratory for the Synthesis and Application of Organic Functional Molecules, Ministry of Education & College of Chemistry & Chemical Engineering, Hubei University, Wuhan 430062, People's Republic of China

dominant {100} facets exhibited superior electrocatalytic activity toward glucose oxidation [13], but the synthesis process is somewhat tedious and difficult [14, 15]. The AuNBPs with two sharp tips is another type of elongated Au nanocrystal and possesses {100} facets. Besides, there are a large fraction of the surface atoms presented on edges and corners of AuNBPs, which may provide more incipient gold oxide. Thus, AuNBPs expect to improve the sensitivity of the sensors.

The aggregation of nanoparticles during the electrocatalytic process lead to decrease the electrocatalytic activity. To overcome this problem, a variety of materials such as polypyrrole (PPy), polyaniline (PANI), reduced graphene oxide (rGO) and MWCNTs have been investigated as the supporting material. Among these materials, MWCNTs have received great interest primarily for their excellent electrical conductivity and large specific surface area [16]. Due to the synergistic effect of AuNBPs and MWCNTs, the electrocatalytic activity of AuNBPs can be further improve.

A electrochemical sensing platform based on AuNBP/MWCNTs is developed to detect glucose and hydrogen peroxide (Scheme 1). The electrochemical sensor shows excellent performance such as outstanding selectivity, high sensitivity, wide linear range, good long-term stability and reproducibility due to the merits of AuNBPs and MWCNTs. Furthermore, it has the possibility of application in real sample analysis.

Material and methods

Chemicals and reagents

Gold(III) chloride trihydrate ($HAuCl_4 \cdot 3H_2O$, ≥49.0% Au basis) was purchased from Sigma-Aldrich (https://www.sigmaaldrich.com/). Sodium citrate dihydrate, sodium borohydride ($NaBH_4$), hexadecyl trimethyl ammonium bromide (CTAB), hydrochloric acid (HCl), silver nitrate ($AgNO_3$), ascorbic acid (AA), hexadecyltrimethylammonium chloride (CTAC), ammonia solution ($NH_3 \cdot H_2O$, 25–28%), hydrogen peroxide solution (30 wt% in H_2O), potassium chloride (KCl), nitric acid (HNO_3), potassium ferricyanide ($K_3[Fe(CN)_6]$), potassium ferrocyanide trihydrate ($K_4[Fe(CN)_6]$), potassium nitrate (KNO_3), D-fructose, saccharose, D-(+)-maltose monohydrate, sodium hydroxide (NaOH), D-(+)-glucose, uric acid (UA), dopamine hydrochloride (DA), 4-Acetamidophenol (AAP), sodium phosphate dibasic dodecahydrate ($Na_2HPO_4 \cdot 12H_2O$), potassium phosphate monobasic (KH_2PO_4), chitosan, and multiwalled carbon nanotubes (MWCNTs, 2~5 nm diameter, 10~30 nm length, >95%) were purchased from Aladdin Biological Technology Co. Ltd. (http://www.aladdin-e.com/). For the detection of hydrogen peroxide, 0.1 M phosphate buffer (PB, pH 7.0) was prepared using $Na_2HPO_4 \cdot 12H_2O$ and KH_2PO_4 without deoxygenation.

Synthesis of gold nanobipyramids (AuNBPs) and preparation of sensors

The AuNBPs were synthesized in aqueous solution by seed-mediated growth methods with minor modification [17, 18]. The experiment details is described in the the ESM.

Before the modification, a glassy carbon electrode (GCE) was polished with 0.05 μm alumina slurry and thoroughly rinsed by ultrasonication in ethanol and deionized water. The AuNBP/MWCNTs were prepared by mixing MWCNTs (2.3 mg) with AuNBPs suspension (500 μL) under the ultrasound condition. 20 μL of the well dispersed suspension was dropped onto the polished GCE. After drying, 4 μL of chitosan solution (0.5%) was dropped onto the modified GCE. The AuNBPs or MWCNTs modified GCE prepared under the same conditions were used as control.

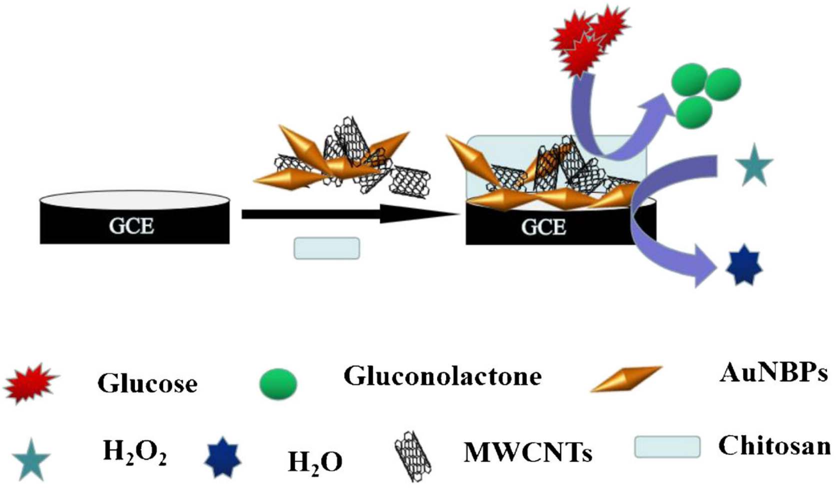

Scheme 1 Schematic illustration of the AuNBP/MWCNT nanocomposites that were used to modify a glassy carbon electrode (GCE) for the detection of glucose and hydrogen peroxide

Apparatus and electrochemical measurements

The preparation process of the AuNBPs were tested by UV-vis spectrum (UV-vis, PERSEE TU-1901). The morphologies of the AuNBPs were investigated by field emission scanning electron microscopy (FESEM, HITACHI SU8010). The crystal structure of the prepared AuNBPs were testified by X-ray diffraction patterns (XRD, Bruker D8 Advance) with Cu K_{α} radiation. X-ray photoelectron spectroscopy (XPS, ESCALAB 250Xi) with Al K_{α} source was employed to analyse the composition of AuNBPs.

The CHI 660E electrochemical workstation equipped with three-electrode arrangement was employed to conduct the electrochemical measurements. The working electrode was the AuNBPs, MWCNTs or AuNBP/MWCNTs modified GCE. The Pt foil and a saturated calomel electrode (SCE) served as the counter electrode and the reference electrode, respectively. All potentials are reported with respect to the SCE throughout this paper.

Results and discussion

Choice of materials

The irregular morphologies of AuNPs with more corners and edges result in more incipient gold oxide, which may act as a fast redox mediator for the oxidation of glucose [19]. It was report that glucose oxidation is strongly dependent on the shape of Au nanocrystals and {100} facets of Au nanocrystals are significantly more active for glucose oxidation. What's more, Au nanocrystal catalysts exhibit remarkably high stability during the electrocatalytic oxidation process [13]. So, the AuNBPs are expected to be a promising electrocatalyst. To further improve the sensitivity of the sensor, MWCNTs with excellent conductivity are used as supporter to form nanocomposites with AuNBPs.

Characterization of the gold nanobipyramids (AuNBPs)

As shown in Fig. S1(A) and Fig. S1(B), the AuNBPs with uniform size about 76 nm are well dispersed, and there are a small amount of AuNPs about 50 nm coupling with the AuNBPs. This phenomenon is consistent with the result of UV-vis spectrum (Fig. S1(C)). For comparison, the AuNRs about 51 nm are also synthesized (Fig. S2). The crystallinity was investigated by XRD, as shown in Fig. 1(a). For the two typers of nanoparticles, the peaks positioned at 38.2°, 44.2°, 64.4°, 77.4° and 81.5° correspond to the (111), (200), (220), (311) and (222) plane of face-centered cubic (fcc) of Au, respectively. What's more, the intensity ratios of (200) to (111) planes for AuNBPs and AuNRs are 0.62 and 0.51, respectively. This indicates that AuNBPs have more {100} facets than that of AuNRs.

Electrochemical characterization

As shown in Fig. 1(b), the cyclic voltammetry (CV) in 0.5 M H_2SO_4 solution was conducted to investigate the electrochemical behaviors. Both of the AuNBPs (b), AuNBP/MWCNTs (c) and AuNRs (e) exhibit significant electro-chemical responses similar to the bulk Au electrode (d), which correspond to the signatures of polycrystalline Au in acidic medium. The reduction peak current at +0.90 V of AuNBPs is 14 times as much as that of the bulk Au electrode, indicating that the electrocatalytic activity and surface area of the AuNBPs are bigger than those of bulk Au [20]. What's more, the reduction peak current increases significantly for introducing the MWCNTs into the AuNBPs to form nanocomposites. It suggest that the AuNBP/MWCNTs can enhance the electron transfer rate due to the synergistic effect between AuNBPs and MWCNTs thus improve the sensitivity of the electrochemical sensor [5, 21].

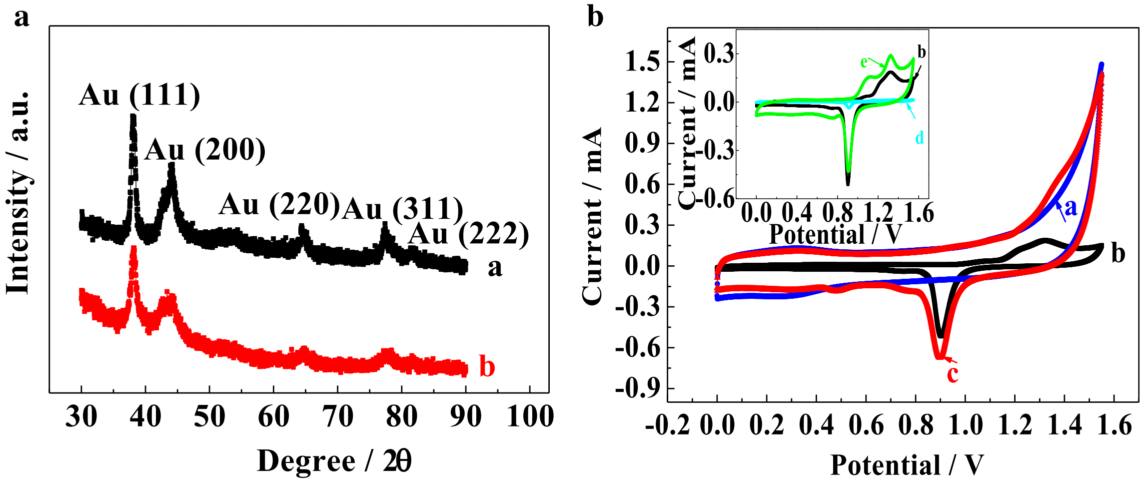

Fig. 1 **a** XRD of AuNBPs (a) and AuNRs (b); **b** The CVs of the MWCNTs (a), AuNBPs (b), AuNBP/MWCNTs (c), bulk Au electrode (d) and AuNRs (e) in N_2-saturated 0.5 mM H_2SO_4 at scan rate of 50 mV/s

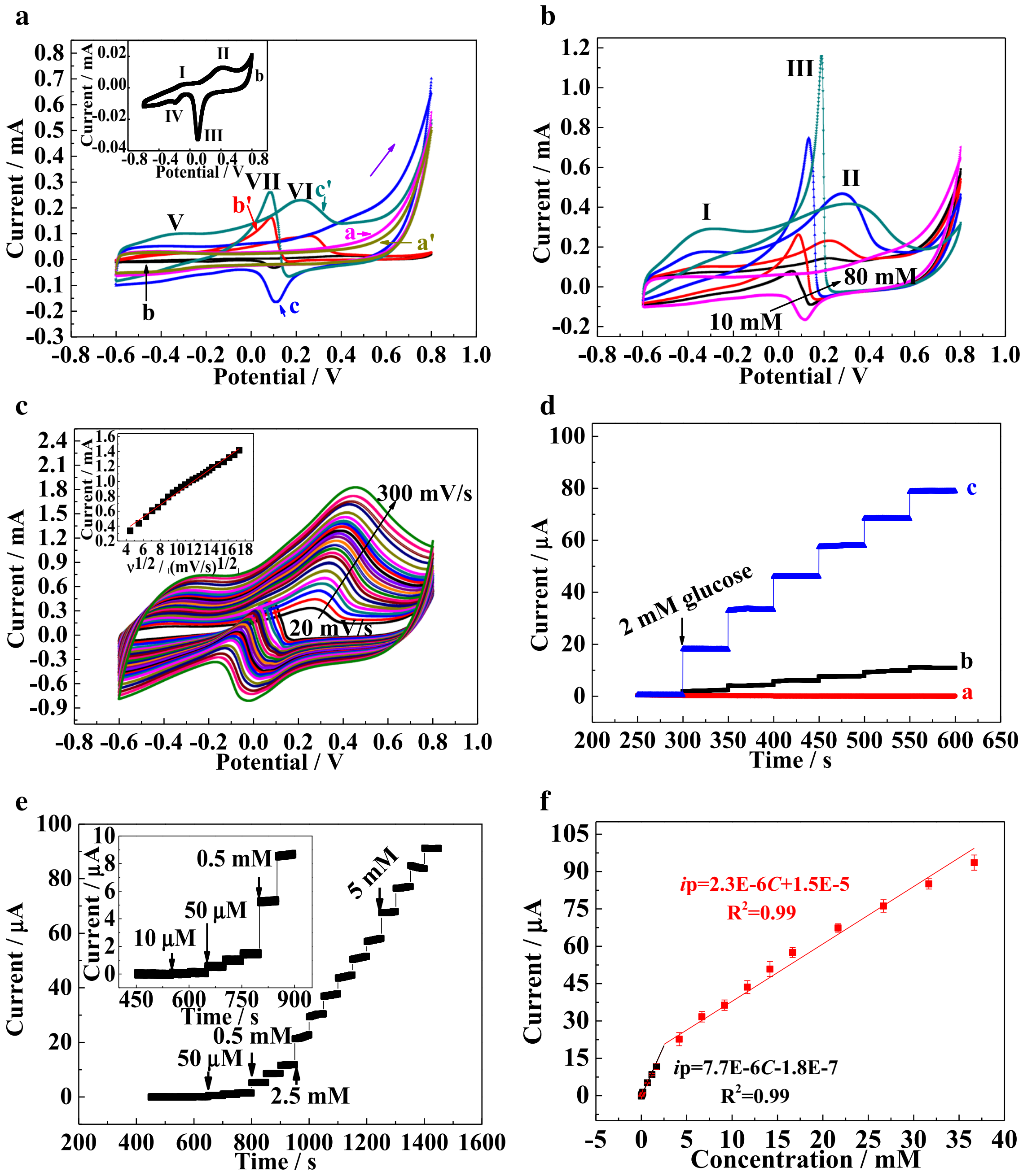

Fig. 2 **a** The CVs of the MWCNTs (a, a'), AuNBPs (b, b'), AuNBP/MWCNTs (c, c') in 0.1 M NaOH with (a', b', c') and without (a, b, c) 20 mM glucose; **b** The CVs of the AuNBP/MWCNTs in 0.1 M NaOH containing different concentration of glucose; **c** The CVs of the AuNBP/MWCNTs in 0.1 M NaOH with 20 mM glucose at various scan rates, Insert: The calibration curve of current vs. square root of scan rate; **d** Amperometric response of the MWCNTs (a), AuNBPs (b), AuNBP/MWCNTs (c) at +0.15 V; **e** Amperometric response of the AuNBP/MWCNTs at +0.15 V with successive additions of different concentrations of glucose; **f** Dependence of the current as a function of the glucose concentration

Response to glucose

The oxidation of glucose is strongly dependent on the number of AuOH sites [13]. As shown in Fig. S3(A), the oxidation current of AuNBP/MWCNTs toward glucose in 0.1 M NaOH is bigger than that in 0.1 M PB. This indicates that there are more AuOH sites in alkaline solution. Consequently, 0.1 M NaOH is chosen as electrolyte to improve the electrocatalytic activity of AuNBP/MWCNTs. As shown in Fig. 2 (a), the CVs of MWCNTs (a, a'), AuNBPs (b, b'), and AuNBP/MWCNTs (c, c') modified electrode in 0.1 M NaOH solution with (a', b', c') or without (a, b, c) 20 mM glucose were conducted. For the MWCNTs (a, a'), no redox peaks are observed with or without glucose, indicating that the

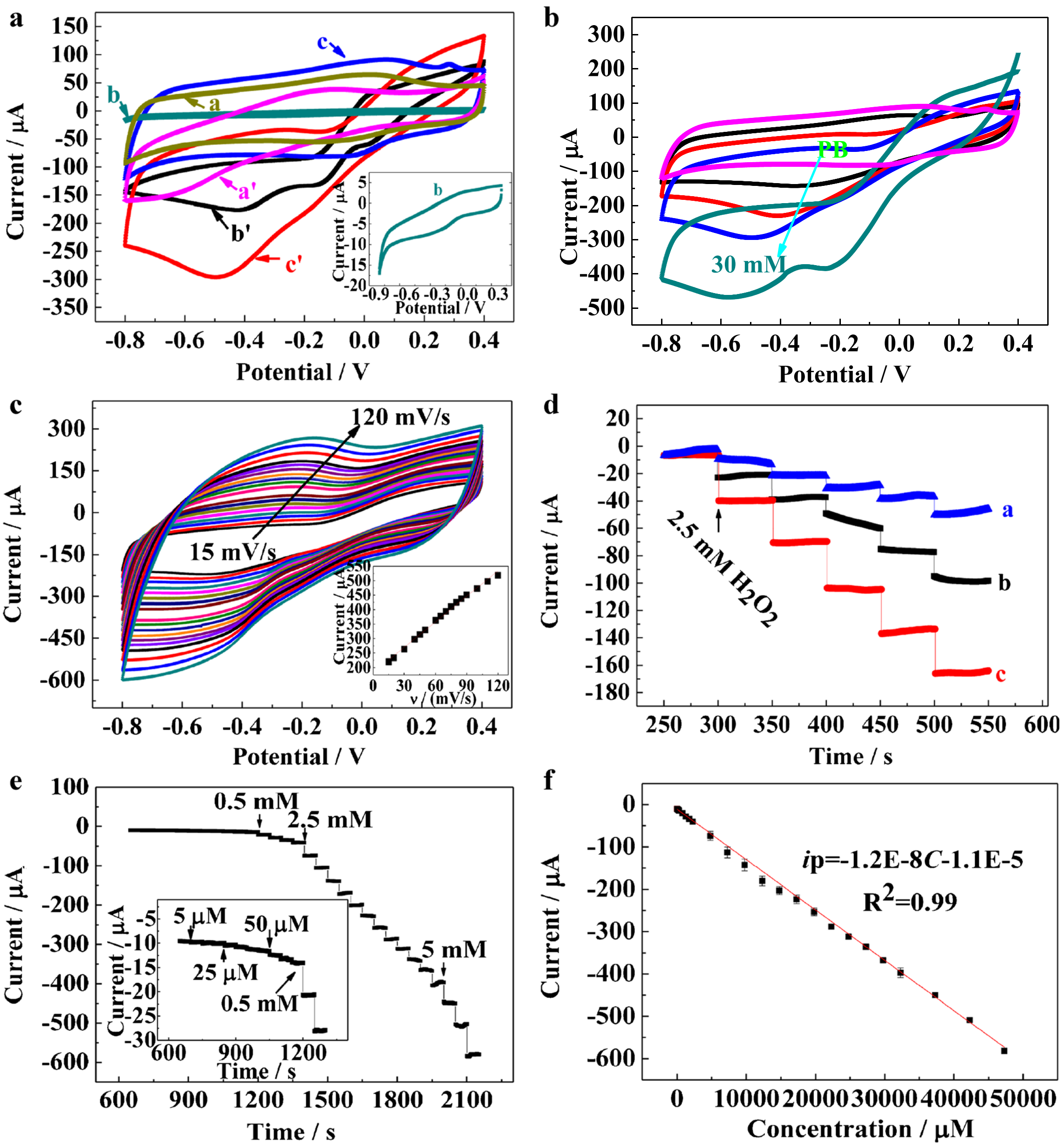

Fig. 3 **a** The CVs of the MWCNTs (a, a'), AuNBPs (b, b'), AuNBP/MWCNTs (c, c') in 0.1 M PB with (a', b', c') and without (a, b, c) 15 mM H_2O_2; **b** The CVs of the AuNBP/MWCNTs in 0.1 M PB containing different concentration of H_2O_2; **c** The CVs of the AuNBP/MWCNTs in 0.1 M PB with 15 mM H_2O_2 at various scan rates, Insert: The calibration curve of current vs. scan rate; **d** Amperometric response of the MWCNTs (a), AuNBPs (b), AuNBP/MWCNTs (c) at −0.50 V; **e** Amperometric response of the AuNBP/MWCNTs at −0.50 V with successive additions of different concentrations of H_2O_2; **f** Dependence of the current as a function of the H_2O_2 concentration

overpotential of glucose oxidation at MWCNTs is high. The electrochemical behavior of AuNBP/MWCNTs (c) in 0.1 M NaOH without glucose is similar to that of AuNBPs (b). The peak I (−0.10 V) and peak II (+0.40 V) are attributed to the oxidation of AuNBPs to form AuOH by the adsorbed OH^- and the formation of Au oxides by the oxidation of AuOH, respectively. The cathodic peak around +0.10 V (peak III) is attributed to the reduction of Au oxides to AuOH, and the peak at −0.19 V (IV) resulted from the reduction of AuOH into AuNBPs [22]. It is worth noticing that there are many differences occurred with 20 mM glucose for AuNBPs (b') and AuNBP/MWCNTs (c'). In the positive scan, the peak V and VI are attributed to the oxidation of glucose to dehydrogenated glucose, and subsequently to gluconolactone. As the potential goes to more positive, the current decreases due to the formation of Au oxides [19]. Whereas in the negative scan, a sharp peak (VII) is attributed to the oxidation of glucose resulting from the reduction of the Au oxides [23]. What's more, the oxidation current of AuNBP/MWCNTs is bigger than that of AuNBPs and the oxidation potential (peak

VI) shifts more than 50 mV toward negative potential as compared to that of AuNBPs. It reveals that the AuNBP/MWCNTs can enhance the electrocatalytic activity and decrease the overpotential of glucose oxidation. It is shown in Fig. S3(B) that the AuNBPs show better electrocatalytic activity than that of AuNRs. This because more {100} facets and incipient gold oxide are available in AuNBPs. As shown in Fig. 2(b), when the glucose concentration increase from 10 to 80 mM, the peak current of glucose oxidation (I, II, III) gradually increase. It indicates that the electrochemical sensor based on AuNBP/MWCNTs can be used to detect of glucose with good sensitivity.

A further investigation of glucose oxidation on AuNBP/MWCNTs was conducted by CVs in 0.1 M NaOH with 20 mM glucose at different scan rates from 20 to 300 mV/s. Obviously, the peak current increases along with the increasing applied scan rate and the current has linear relation with the square root of the scan rate (Fig. 2(c)). This indicates that the glucose electro-oxidation at the AuNBP/MWCNTs is a diffusion-controlled process.

For the amperometric method used to detect glucose, the working potential is crucial to obtain high sensitivity and good selectivity. As shown in Fig. S4(A), +0.15 V is selected as the optimal working potential for further use. After each addition of 2 mM glucose, a stepwise current response is observed. The response time reaching 95% of the steady-state current is less than 2 s for the excellent electrocatalytic activity of AuNBP/MWCNTs. It is shown in Fig. 2(d), the current of the AuNBP/MWCNTs towards 2 mM glucose is bigger than that of AuNBPs and MWCNTs at +0.15 V, which agrees with the result of CVs.

Under +0.15 V, the linear relationship of AuNBP/MWCNTs is obtained by the successive addition of glucose (Fig. 2(e)). As shown in Fig. 2(f), the current response increases linearly along with the glucose concentration from 10 μM to 36.7 mM, which covers the normal physiological glucose level of 4.4–6.6 mM [24]. The sensitivity and limit of detection (LOD) of the sensor towards glucose is 101.2 μA mM^{-1} cm^{-2} and 3.0 μM ($S/N = 3$), respectively. Compared with other non-enzymatic glucose sensors, the advantages of the sensor based on AuNBP/MWCNTs are the wider linear range and the sensitivity warrant further improvement (Table S1). The good performance of AuNBP/MWCNTs might result from more incipient gold oxide provided by the AuNBPs and the synergistic effect of AuNBPs and MWCNTs.

Response to hydrogen peroxide

As shown in Fig. 3(a), no obvious redox peaks is observed at all the modified electrodes without hydrogen peroxide. In presence of 15 mM hydrogen peroxide, no reduction peak is observed at MWCNTs (a'). This suggests that the electro-reduction of hydrogen peroxide on MWCNTs required a large overpotential. There is a reduction peak appeared at AuNBPs (b') and AuNBP/MWCNTs (c') around −0.50 V, which is ascribed to reduction of hydrogen peroxide. The peak current of AuNBP/MWCNTs is bigger than that of AuNBPs. In addition, the peak current originating from the hydrogen peroxide reduction increases along with the concentration of hydrogen peroxide (Fig. 3(b)). The results demonstrate that hydrogen peroxide is easily reduced on AuNBP/MWCNTs due to the excellent electrocatalytic activity of AuNBP/MWCNTs. Furthermore, the hydrogen peroxide reduction on the AuNBP/MWCNTs is a surface-controlled process (Fig. 3(c)).

It is shown in Fig. S4(B), −0.50 V is selected as optimal working potential. Moreover, the amperometric response of AuNBP/MWCNTs at −0.50 V is the highest. It indicates that the electrocatalytic activity of the AuNBP/MWCNTs towards hydrogen peroxide reduction is the best (Fig. 3(d)). The

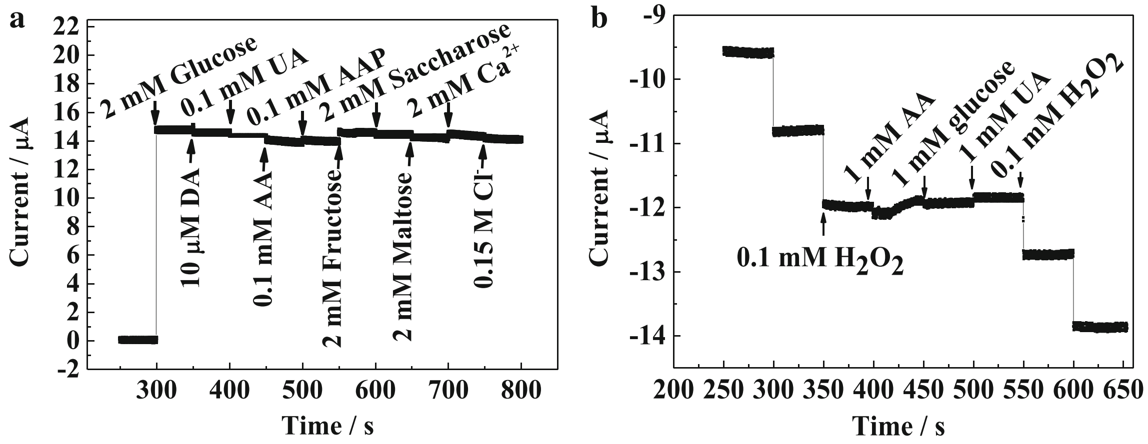

Fig. 4 **a** Amperometric response of the AuNBP/MWCNTs at +0.15 V toward glucose (2 mM), DA (10 μM), UA/AA/AAP (0.1 mM), fructose/saccharose/maltose/Ca^{2+} (2 mM) and Cl^{-} (0.15 M); **b** Amperometric response of the AuNBP/MWCNTs at −0.50 V toward H_2O_2 (0.1 mM), AA/glucose/UA (1 mM)

Table 1 Non-enzymatic glucose sensor based on AuNBP/MWCNTs was applied to detect the concentration of glucose in human serum and hydrogen peroxide in hydrogen peroxide-based antibacterial lotion (3%)

	Number	Detected by our sensor (mM)	Detected by glucometer (mM)	Added (mM)	Found (mM)	RSD (%)	Recovery (%)
Glucose	1	5.32	5.43	5.00	10.2	2.3	98.8
	2	4.96	5.12	10.0	15.3	3.7	102.3
	3	5.27	5.39	15.0	20.0	2.8	98.7
Hydrogen peroxide	1	2.39	/	1.00	3.43	3.5	101.2
	2	2.28	/	5.00	7.14	2.4	98.1
	3	2.34	/	10.0	12.2	1.9	98.9

reduction current response increases along with the concentration of hydrogen peroxide under −0.50 V (Fig. 3(e)). It exhibits a good linear range from 5.0 μM to 47.3 mM with a LOD of 1.5 μM and the sensitivity of 170.6 μA mM^{-1} cm^{-2} (Fig. 3(f)). Compared with other non-enzymatic electrochemical sensors for detection of hydrogen peroxide, the results are comparable or even better than other reports (Table S2).

Selectivity, reproducibility and stability

The good selectivity, reproducibility and stability of sensors are the key factors for practical application. For glucose detection, DA, UA, AA, AAP, fructose, saccharose, maltose, Ca^{2+} and Cl^- may interfere the accurate detection of glucose [25, 26]. As shown in Fig. 4(a), the addition of 10 μM DA, 0.1 mM UA/AA/AAP, 2 mM fructose/saccharose/maltose/Ca^{2+} and 0.15 M Cl^- into 0.1 M NaOH results in negligible signal changes compared with that of 2 mM glucose. This suggests that the electrochemical sensor based on AuNBP/MWCNTs for glucose detection have a good selectivity. It was reported that the oxidation of the co-existing reducing species on Au-based modified electrode usually occurs at +0.30 to +0.40 V [27]. The lower working potential (+0.15 V) contributes to the excellent selectivity. Furthermore, the alkaline electrolyte can minimize the interference from the co-existing reducing species by providing a restricted environment [28]. It is shown in Fig. 4(b), the non-enzymatic electrochemical sensor also exhibits excellent selectivity for hydrogen peroxide detection.

The current responses of five-paralleled electrodes towards 2 mM glucose and 2.5 mM hydrogen peroxide are recorded and the relative standard deviation (RSD) is 2.3% (Fig. S5 (A)) and 3.5% (Fig. S5 (B)), respectively. This demonstrated that the sensor have a good reproducibility. In addition, the current response still retain up to 98.0% of the original value for glucose (Fig. S5(C)) and 94.7% for hydrogen peroxide (Fig. S5(D)) after 30 days of storage in air at room temperature, which demonstrates the satisfactory stability of the sensor.

Real sample analysis

The feasibility of the sensor is testified by detecting of the concentration of glucose in human serum and hydrogen peroxide in hydrogen peroxide-based antibacterial lotion (3%), respectively. The glucose concentration in human serum detected by our resultant sensor agrees with the results detected by glucometer (ONE TOUCH Ultra, LIFESCAN) and the concentration of hydrogen peroxide in hydrogen peroxide-based antibacterial lotion (3%) detected by our resultant sensor is consistent with the mark (2.49 mM). As listed in Table 1, the non-enzymatic sensor is demonstrated to be feasible for practical application with acceptable recovery and RSD.

Conclusions

A non-enzymatic electrochemical sensor on the basis of using AuNBP/MWCNTs as an efficient electrode material has been developed to detect of glucose in human serum and hydrogen peroxide in hydrogen peroxide-based antibacterial lotion (3%). The sensor possess excellent sensitivity, good selectivity, high reproducibility and stability. The outstanding performance of the sensor is ascribed to the synergistic effect and more incipient gold oxide provided by the AuNBPs. The major limitation of the sensor for detection of glucose is that it need to work in strong alkaline solution.

Acknowledgements This work was partially supported by the Natural Science Foundation of China (81573110, 31270958), the Chinese National 863 plan (2012AA02A407), the Natural Science Foundation of Zhejiang Province (LY14H190004, LY13H100003, LY15H160066), the Key Science and Technology Innovation Team of Zhejiang Province, Wenzhou Municipal Research Program (Y20160009, Y20160074), and Natural Science Foundation of Zhejiang Province (LQ17B030003).

Compliance with ethical standards The author(s) declare that they have no competing interests.

References

1. Wang CH, Yang CH, Chang JK (2017) High-selectivity electrochemical non-enzymatic sensors based on graphene/Pd nanocomposites functionalized with designated ionic liquids. Biosens Bioelectron 89:483–488. https://doi.org/10.1016/j.bios.2016.03.071
2. Dhara K, Mahapatra DR (2018) Electrochemical nonenzymatic sensing of glucose using advanced nanomaterials. Microchim Acta 185:49–81. https://doi.org/10.1007/s00604-017-2609-1
3. Yu ZY, Li HJ, Zhang XM, Liu NK, Tan WL, Zhang X, Zhang LL (2016) Facile synthesis of $NiCo_2O_4$@polyaniline core-shell nanocomposite for sensitive determination of glucose. Biosens Bioelectron 75:161–165. https://doi.org/10.1016/j.bios.2015.08.024
4. Zhong SL, Zhuang JY, Yang DP, Tang DP (2017) Eggshell membrane-templated synthesis of 3D hierarchical porous Au networks for electrochemical nonenzymatic glucose sensor. Biosens Bioelectron 96:26–32. https://doi.org/10.1016/j.bios.2017.04.038
5. Kangkamano T, Numnuam A, Limbut W, Kanatharana P, Thavarungkul P (2017) Chitosan Cryogel with embedded gold nanoparticles decorated multiwalled carbon nanotubes modified electrode for highly sensitive flow based non-enzymatic glucose sensor. Sensors Actuators B Chem 246:854–863. https://doi.org/10.1016/j.snb.2017.02.105
6. Fu YY, Liang FF, Tian HF, Hu JB (2014) Nonenzymatic glucose sensor based on ITO electrode modified with gold nanoparticles by ion implantation. Electrochim Acta 120:314–318. https://doi.org/10.1016/j.electacta.2013.12.082
7. Luo Y, Kong FY, Li C, Shi JJ, Lv WX, Wang W (2016) One-pot preparation of reduced graphene oxide-carbon nanotube decorated with Au nanoparticles based on protein for non-enzymatic electrochemical sensing of glucose. Sensors Actuators B Chem 234:625–632. https://doi.org/10.1016/j.snb.2016.05.046
8. Guo XM, Deng HM, Zhou H, Fan TX, Gao ZQ (2015) Detection of glucose with a lamellar-ridge architectured gold modified electrode. Sensors Actuators B Chem 206:721–727. https://doi.org/10.1016/j.snb.2014.09.019
9. Tang YR, Liu Q, Yang X, Wei M, Zhang MX (2017) Copper oxide coated gold nanorods like a film: A facile route to nanocomposites for electrochemical application. J Electroanal Chem 806:8–14. https://doi.org/10.1016/j.jelechem.2017.10.032
10. Pang P, Yang Z, Xiao S, Xie J, Zhang Y, Gao Y (2014) Nonenzymatic amperometric determination of hydrogen peroxide by graphene and gold nanorods nanocomposite modified electrode. J Electroanal Chem 727:27–33. https://doi.org/10.1016/j.jelechem.2014.05.028
11. Li QQ, Cui SZ, Yan XL (2012) Electrocatalytic oxidation of glucose on nanoporous gold membranes. J Solid State Electrochem 16:1099–1104. https://doi.org/10.1007/s10008-011-1501-x
12. Tang Y, Cheng WL (2013) Nanoparticle-modified electrode with size- and shape-dependent electrocatalytic activities. Langmuir 29:3125–3132. https://doi.org/10.1021/la304616k
13. Wang JF, Gong JX, Xiong YS, Yang JD, Gao Y, Liu YL, Lu XQ, Tang ZY (2011) Shape-dependent electrocatalytic activity of monodispersed gold nanocrystals toward glucose oxidation. Chem Commun 47:6894–6896. https://doi.org/10.1039/c1cc11784j
14. Wu HL, Kuo CH, Huang MH (2010) Seed-mediated synthesis of gold nanocrystals with systematic shape evolution from cubic to trisoctahedral and rhombic dodecahedral structures. Langmuir 26:12307–12313. https://doi.org/10.1021/la1015065
15. Niu WX, Zheng SL, Wang DW, Liu XQ, Li HJ, Han S, Chen J, Tang ZY, Xu GB (2009) Selective synthesis of single-crystalline rhombic dodecahedral, octahedral, and cubic gold nanocrystals. J Am Chem Soc 131:697–703. https://doi.org/10.1021/ja804115r
16. He ZY, Zang SA, Liu Y, He Y, Lei HT (2015) A multi-walled carbon nanotubes-poly(L-lysine) modified enantioselective immunosensor for ofloxacin by using multi-enzyme-labeled gold nanoflower as signal enhancer. Biosens Bioelectron 73:85–92. https://doi.org/10.1016/j.bios.2015.05.054
17. Li Q, Zhuo XL, Li S, Ruan QF, Xu QH, Wang JF (2015) Production of monodisperse gold nanobipyramids with number percentages approaching 100% and evaluation of their Plasmonic properties. Adv Opt Mater 3:801–812. https://doi.org/10.1002/adom.201400505
18. Feng J, Chen LM, Xia YZ, Xing J, Li ZH, Qian QP, Wang Y, Wu AG, Zeng LY, Zhou YL (2017) Bioconjugation of gold nanobipyramids for SERS detection and targeted photothermal therapy in breast cancer. ACS Biomater Sci Eng 3:608–618. https://doi.org/10.1021/acsbiomaterials.7b00021
19. Karra S, Wooten M, Griffith W, Gorski W (2016) Morphology of gold nanoparticles and electrocatalysis of glucose oxidation. Electrochim Acta 218:8–14. https://doi.org/10.1016/j.electacta.2016.09.097
20. Han L, Zhang S, Han L, Yang DP, Hou C, Liu A (2014) Porous gold cluster film prepared from Au@BSA microspheres for electrochemical nonenzymatic glucose sensor. Electrochim Acta 138:109–114. https://doi.org/10.1016/j.electacta.2014.06.095
21. Liu X, Mao LG, Wang YL, Shi XB, Liu Y, Yang Y, He Z (2016) Electrochemical sensor based on imprinted sol-gel polymer on Au NPs-MWCNTs-CS modified electrode for the determination of acrylamide. Food Anal Methods 9:114–121. https://doi.org/10.1007/s12161-015-0172-0
22. Xu ML, Song YH, Ye YH, Gong CC, Shen Y, Wang LY, Wang L (2017) A novel flexible electrochemical glucose sensor based on gold nanoparticles/polyaniline arrays/carbon cloth electrode. Sensors Actuators B Chem 252:1187–1193. https://doi.org/10.1016/j.snb.2017.07.147
23. Nantaphol S, Watanabe T, Nomura N, Siangproh W, Chailapakul O, Einaga Y (2017) Bimetallic Pt-Au nanocatalysts electrochemically deposited on boron-doped diamond electrodes for nonenzymatic glucose detection. Biosens Bioelectron 98:76–82. https://doi.org/10.1016/j.bios.2017.06.034
24. Wang J (2008) Electrochemical glucose biosensors. Chem Rev 108:814–825. https://doi.org/10.1021/cr068123a
25. Han L, Yang DP, Liu AH (2015) Leaf-templated synthesis of 3D hierarchical porous cobalt oxide nanostructure as direct electrochemical biosensing interface with enhanced electrocatalysis. Biosens Bioelectron 63:145–152. https://doi.org/10.1016/j.bios.2014.07.031
26. Tang Y, Liu Q, Jiang Z, Yang X, Wei M, Zhang M (2017) Nonenzymatic glucose sensor based on icosahedron AuPd@CuO core shell nanoparticles and MWCNT. Sensors Actuators B Chem 251:1096–1103. https://doi.org/10.1016/j.snb.2017.05.090
27. Łuczak T, Bełtowska-Brzezinska M (2011) Gold electrodes modified with gold nanoparticles and thio compounds for electrochemical sensing of dopamine alone and in presence of potential interferents. A comparative study. Microchim Acta 174:19–30. https://doi.org/10.1007/s00604-011-0614-3
28. Soomro RA, Akyuz OP, Ozturk R, Ibupoto ZH (2016) Highly sensitive non-enzymatic glucose sensing using gold nanocages as efficient electrode material. Sensors Actuators B Chem 233:230–236. https://doi.org/10.1016/j.snb.2016.04.065